AUTOMATED TRANSMISSION LINE FAULT ANALYSIS USING SYNCHRONIZED SAMPLING AT TWO ENDS

M. Kezunović, Senior Member,
Texas A&M University
College Station, Texas, U. S. A.

B. Peruničić*
Lamar University
Beaumont, Texas, U. S. A.

Abstract– This paper introduces a new approach to fault analysis using synchronized sampling. A digital fault recorder with Global Positioning System (GPS) satellite receiver is the source of data for this approach. Fault analysis functions, such as fault detection, classification and location are implemented for a transmission line using synchronized samples from two ends of a line. This technique can be extremely fast, selective and accurate, providing fault analysis performance that can not easily be matched by other known techniques.

Keywords: Fault Analysis, Fault Detection, Fault Classification, Fault Location, Synchronized Sampling

INTRODUCTION

Automated fault analysis is of interest to operators and protection engineers alike for different reasons. The operators needed to confirm and isolate the faulted sections before any system restoration is attempted. Protection engineers need to fully explain fault events and evaluate operation of relaying equipment in order to report any misoperations. Both groups can, therefore, benefit from selective and accurate techniques for fault analysis. Automating this process brings an improvement in the time response which is also quite desirable. Attempts to automate fault analysis date back to 1969 [1].

This paper reports on a continuing development of automated transmission line fault analysis techniques at Texas A&M University. The initial development utilized an expert system approach for analysis of operation of relays, circuit breakers and communication channels. A signal processing technique was utilized in this development for detection and classification of faults [2]. A prototype of an automated fault analysis system has been installed in a substation with support from Houston Lighting and Power Company [3]. Further improvements were aimed at providing more selective fault detection and classification using neural network technologies [4]. Finally, a new fault location technique has been developed to increase the overall performance of the fault analysis [5]. The new fault location technique is based on time domain solution of transmission line equations obtained by directly solving the equations for each data sampling instant. This requires samples of voltages and currents at both ends of the line taken synchronously. The computational burden is reduced when compared to some other fault location techniques also requiring data from two ends [5–8]. The accuracy is comparable, and in some cases, even improved.

This paper describes an implementation of the fault detection, classification and location steps which provide an improvement of the automated fault analysis approach developed earlier. The new technique is extremely accurate and provides robust results even under quite difficult constraints such as time varying fault resistance. The computational burden and implementation complexity are significantly reduced. This solution can be provided as an add-on to a standard digital fault recorder equipped with a Global Positioning System (GPS) satellite receiver providing the synchronized sampling [9].

The technique proposed in this paper is based on a lumped parameter transmission line model and is applicable to the situation where the shunt capacitances can be neglected. A traveling wave based fault detection and classification, as well as an implementation of a dedicated data sampling synchronization system have been described by other authors [10,11]. The approach presented in this paper can also be extended to consideration of the distributed parameter transmission line model with an accurate fault location technique included [5]. This addition of an accurate fault location can be viewed as a major enhancement of the previously considered synchronizing sampling techniques developed based on the traveling wave methods [10,11]. This makes the concept described in this paper applicable for both short and long transmission lines with capacitances either excluded from or included in the line models.

This first part of the paper describes theoretical considerations of the algorithm. A simplified model representing a short transmission line is used as an example. The next section provides implementation details for the new fault detection, classification and location approach. Extensive EMTP simulation results used to illustrate the performance are given at the end.

THEORETICAL BASIS

The transmission line considered in this section has a length l and is homogeneous to simplify the presentation. As mentioned earlier, the assumptions can easily be extended to include distributed parameter transmission line models with capacitance included [5,9]. For the simplified consideration, conductance and capacitance are neglected. One line representation of the 3-phase

*The work was done while the author was with Texas A&M University.

0-7803-2663-6/95 $4.00 © 1995 IEEE

line, with a fault at the distance x from the end S, is represented in Fig. 1.

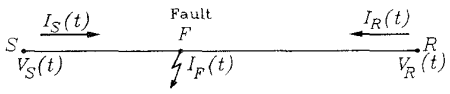

Fig. 1. One Line Representation of the 3–Phase Transmission Line

Detection, classification and location of the fault are based on two vectors defined as:

$$\Delta I(t) = I_S(t) + I_R(t) \tag{1}$$

$$\Delta V(t) = V_S(t) - V_R(t) + l\left[RI_R(t) + L\frac{dI_R(t)}{dt}\right] \tag{2}$$

$V_S(t),\ V_R(t)$	–	Vectors of Phase Voltages
$I_S(t),\ I_R(t),\ I_F(t)$	–	Vectors of Phase Currents
S, R	–	Transmission Line Ends
$R,\ L$	–	Matrices of Self and Mutual Line Parameters

In normal operating conditions, the fault current $I_F(t)$ is zero. As a consequence of Kirchhoff's current and voltage laws, the above vectors are equal to zero.

$$\Delta I(t) = 0 \tag{3}$$

$$\Delta V(t) = 0 \tag{4}$$

If the line is faulted, the values of these vectors are:

$$\Delta I(t) = I_F(t) \tag{5}$$

$$\Delta V(t) = x\left[RI_F(t) + L\frac{dI_F(t)}{dt}\right] \tag{6}$$

The fault current may be eliminated from equations (5) and (6) leading to:

$$\Delta V(t) - x\left[R\Delta I(t) + L\frac{d}{dt}\Delta I(t)\right] = 0 \tag{7}$$

The values of the vectors $\Delta V(t)$ and $\Delta I(t)$ [equations (1) and (2)] at times n/f_s, where f_s is the sampling frequency, can be calculated from current and voltage samples:

$$\Delta I_n = I_{Sn} + I_{Rn} \tag{8}$$

$$\Delta V_n = V_{Sn} - V_{Rn} + l[RI_{Rn} + f_s L(I_{Rn} - I_{Rn-1})] \tag{9}$$

Here, V_{Sn}, V_{Rn}, I_{Sn} and I_{Rn} denote vectors of samples taken synchronously at moments n/f_s. It should be noted that the expression for ΔV_n is an approximate one, since the current derivative can not be measured. Here, the derivative is approximated with "backward" approximation.

The discrete version of the equation (7) is obtained using the same approximation for the current derivative:

$$\Delta V_n - x\varphi_n = 0 \tag{10}$$

$$\varphi_n = R\Delta I_n + f_s L(\Delta I_n - \Delta I_{n-1}) \tag{11}$$

Fault Detection

The line is faulted if any of the phase fault currents differ from zero. Since components of the vector ΔI are equal to the phase fault currents, as shown in equation (5), their samples are the most indicative for the detection of the fault. However, the check of individual samples is not convenient, since these values are prone to the noise–like deviation due to the model and measurement imperfections. This is the reason that L_2 norm average over N instants of the of the vector ΔI_n is selected as an indicator of the presence of the fault (see Appendix I). This indicator is denoted T_n and is calculated using a recursive formula:

$$J_{n,m} = J_{n-1,m} + \frac{1}{N}\Delta I_{n,m}^2 - \frac{1}{N}\Delta I_{n-N+1,m}^2 \tag{12}$$

$$m = a, b, c$$

$$T_n = \sum_{m=a,b,c} J_{n,m} \tag{13}$$

The value of T_n is compared to a pre–set value T. If T is exceeded, the line is considered faulted. T should be selected so that it is larger than the maximum value of T_n in normal operating conditions.

Fault Classification

The outcome of the fault classification defines a fault as *ag, bg, cg, abg, acg, bcg, abcg, ab, ac, bc* or *abcg*. The presence of a letter denotes that there is a fault current in the corresponding wire and/or ground path. The components of ΔI_n, denoted $\Delta I_{n,m}$ (m=*a, b, c*) are equal to the phase fault current samples. The samples of the ground fault current are calculated from the following expression:

$$\Delta I_{n,g} = \sum_{m=a,b,c} \Delta I_{n,m} \tag{14}$$

The averaged squares of $\Delta I_{n,m}$ denoted $J_{n,m}$ are already calculated at any sampling instant n for the purpose of the fault detection using recursive formula (12). The same quantities are used to identify the presence of the fault current in a phase. If the classification of the ground fault is required, the average of the squared ground fault current is calculated as:

$$J_{n,g} = J_{n-1,g} + \frac{1}{N}\Delta I_{n,g}^2 - \frac{1}{N}\Delta I_{n-N+1,g}^2 \tag{15}$$

The values of indicators $J_{n,a}$, $J_{n,b}$, $J_{n,c}$, $J_{n,g}$ are compared to some pre–set values. A phase/ground fault is declared if the corresponding average exceeds the pre–set threshold.

Fault Location

The fault location is based on equations (10) and (11). In these equations ΔV_n, ΔI_n and line parameters are known, while the distance x to the fault has to be determined. The number of available scalar equations is equal to $3N$, if the samples are taken at $N+1$ instant. Since the system of equations is an over–determined one, the most suitable way to find x is to apply the Minimum

Least Square method. This method provides the following best estimate of x:

$$x = \frac{\sum_{n=2}^{N+1} \langle \Delta V_n, \varphi_n \rangle}{\sum_{n=2}^{N+1} \langle \varphi_n, \varphi_n \rangle} \qquad (16)$$

where $<\ ,\ >$ denotes the scalar product of vectors.

All the principles of fault analysis presented here are based on the fundamental electrical laws only. Derived expressions are valid for any set of voltages and currents at transmission line ends. Consequently, voltages do not need to be balanced, some phase voltages may even be zero. This makes the method completely independent of power system operating conditions. The transmission line does not have to be transposed. No assumptions about fault currents need to be imposed. The fault resistance may arbitrarily vary in time. Even an inductive component in the fault impedance may be present. This is a unique feature of the presented method.

Since in the selected example, the conductance and capacitance are neglected, the method as derived, is most suitable for shorter lines. As mentioned earlier, the techniques can easily be extended to include the long line representation as well [5]. The inevitable approximation of the current derivative is also an error source.

Fault Analysis Implementation

Since all three functions of the fault analysis need the same data, they may be implemented as a unique software package. A block diagram of the functional organization is given in Fig. 3.

In this scheme, the detection is performed for each new sample. The needed averaging is performed over one–half of a cycle of data in nonlinear unit NF_2. The outputs of this filter are used both for detection and classification. However, the classification is performed only if a fault is detected. The execution of the classification starts when more post fault data are averaged to increase the reliability of the outcome.

The fault location is also initiated by the fault detection. The data needed for the fault location are stored in three buffers. The fault location begins when a sufficient number of post fault data are stored in buffers.

TEST RESULTS

Proposed fault detection, classification and location technique was designed and implemented as a unique fault analysis program. Fault analysis performance was evaluated using Electromagnetic Transients Program (EMTP) generated data [12]. An actual 161 kV power system was modeled using EMTP and was taken as a test system for various fault event simulations. One line diagram of the test system is given in Fig. 4. The transmission line used for testing of the technique is one between busses 2 and 3 and is 13.35 miles long. Test system parameters used for EMTP modeling are also given in Appendix II.

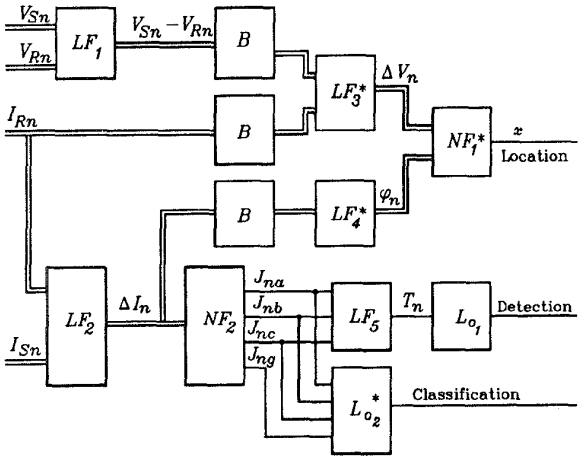

* Triggered by Fault Detection

LF –Linear Filters NF –Nonlinear Filters
L_o –Logic and Comparison B –Buffers
=== –Three (Phases) Quantities___ –Single Quantity

The filter equations are defined as follows:

LF_1 –The difference of two voltages
LF_2 –The equation (8)
LF_3 – The equation (9); start time set by the L_{o1} unit
LF_4 – The equation (11); start time set by the L_{o1} unit
LF_5 –The equation (13)
NF_1–The equation (16)
NF_2–Equations (12) and (15)

The logic units are defined as follows:

L_{o_1} – If $T_n \geq T$, then line is faulted. n – the current discrete time. This unit defines the start of the calculation for the units marked with (*)

L_{o_2} – If $J_{np} \geq J_p$,then p is faulted, $p = a, b, c, g$

Fig. 3. Block Diagram of Fault Analysis Implementation

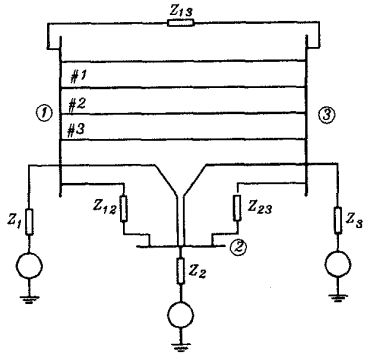

Fig. 4. One Line Diagram of the Test System

Standard criteria selected for the evaluation of fault analysis methods are speed, selectivity and accuracy.

Fault Detection Performance Evaluation

The criterion used for performance evaluation of the detection function is response time of the detection indicator T_n, given by equation (13). The response time of the detection indicator T_n is time that elapses from the fault occurrence to the moment when T_n reaches pre-set threshold T. The response time is expressed as a fraction of the cycle. The value used as a threshold T roughly corresponds to 1kA fault current in a single phase fault.

The response time was observed for several fault cases. They were generated varying the following four simulation parameters: type of the fault, fault location, fault resistance, incidence angle of the fault. Different values of the parameters used in the simulations are shown in Table III.

Phase voltages and currents were sampled at sampling frequency $f_s = 12kHz$. The detection indicator T_n was generated using $\frac{1}{2}$ cycle long window of data.

The results are given in Table IV. They correspond to the test cases obtained for $R_F = 50\Omega$ only, since the times obtained for $R_F = 3\Omega$ cases are smaller. This was expected knowing that T_n is directly proportional to the square of the fault current, and that fault current is inversely proportional to the fault resistance. Response times differ from one fault type to another. The time is smallest for a–b–c–g fault, while largest for a–g fault. This complies with the definition of T_n, T_n being a sum of squares of all phase currents involved in the fault. Incidence angle of the fault influences the response time, too. It is always larger in case of 90°, but never more than 3 times. At the end, it can be seen that the response time is the largest for the faults located in the middle of the line, decreasing its value as the location of the fault moves towards the line ends.

The response time of the detection indicator T_n also depends on the threshold used. The higher the threshold T, the higher response time. Results presented here are obtained for a quite high value of T which represents a rather conservative test case. Nevertheless, the response time varies from 0.02 cycle (best) to 0.330 cycle in the worst case.

Fault Classification Performance Evaluation

For performance evaluation of the classification function, four indicators $J_{n,m}$ for $m = a, b, c, g$ were calculated. Each of the indicators corresponds to one of the phases or ground path, as defined in equations (12) and (15). A criterion used for comparison was selectivity of the classification indicators at the time $t = \frac{3}{2}$ cycle after the fault occurrence.

The test cases used for the performance evaluation of the classification function are the same as the ones used for the evaluation of the detection function. $J_{n,m}$ values were calculated using the $\frac{1}{2}$ cycle window of data. The whole window of data contained 1 cycle of pre-fault and 2 cycles of post-fault data.

It was observed that the classification indicators are very selective and do not differ significantly from location to location, nor for different incidence angles. Values obtained for $R_F = 3\Omega$ are larger than ones for $R_F = 50\Omega$ due to the larger fault current corresponding to smaller R_F. Results obtained for the location of 50%, $R_F = 50\Omega$, and incidence angle 90°, given in Table V, are typical.

Table III. Simulation Parameters

Type of the Fault	a–g, a–b–c–g, b–c, b–c–g
Fault Location	10%, 50%, 80%
Fault Resistance	3Ω, 50Ω
Incidence Angle	0°, 90°

Table IV. Response Time of the Detection Indicator T_n (Fraction of a Cycle)

Locat.	Incid. Angle	Type of the Fault			
		a–g	a–b–c–g	b–c	b–c–g
10%	90°	0.325	0.050	0.165	0.125
	0°	0.150	0.025	0.060	0.045
50%	90°	0.330	0.055	0.170	0.135
	0°	0.165	0.030	0.065	0.050
80%	90°	0.315	0.040	0.155	0.115
	0°	0.155	0.020	0.050	0.040

Table V. Classification Indicators $J_{n,m}(m = a, b, c, g)$

Classif. Indic.	Type of Fault			
	a–g	a–b–c–g	b–c	b–c–g
$J_{n,a}$	$3.4523 \cdot 10^6$	$2.3698 \cdot 10^8$	0	0
$J_{n,b}$	0	$4.0139 \cdot 10^8$	$1.0187 \cdot 10^7$	$2.9814 \cdot 10^8$
$J_{n,c}$	0	$1.1315 \cdot 10^8$	$1.0187 \cdot 10^7$	$2.7424 \cdot 10^8$
$J_{n,g}$	$3.4523 \cdot 10^6$	0.0028	$1.7021 \cdot 10^{-5}$	$8.8414 \cdot 10^5$

For various fault types, values of classification indicators $J_{n,m}$ vary differently with time. For the faults that involve one or two phases and/or ground path, classification indicators of corresponding phases (ground path) establish the steady value soon after the fault occurrence. In case of the three phase to ground fault, classification indicators oscillate with time. Still, the minimum value they reach is of the order of maximum of the other faults classification indicators. The waveforms of classification indicators for a–b–c–g fault and b–c–g fault are given in Fig. 5 and Fig. 6, respectively. Again, it can be observed that these indicators are very selective since their values are distinctively different for various fault types.

Fault Location Performance Evaluation

The criterion used for evaluation of the performance was an error of fault location defined as:

$$\text{error } (\%) = \frac{|\text{actual location} - \text{calculated location}|}{\text{total line length}} \tag{17}$$

A number of various fault events were simulated for testing the fault location function. The time step used for EMTP simulations was $\Delta t = 41.667\mu s$ ($f_{EMTP} =$

Table VI. Error (%) for Location 10%, 50% and 80%

Type of the Fault	Incid. Angle	10%			50%			80%		
		24KHz	12KHz	6KHz	24KHz	12KHz	6KHz	24KHz	12KHz	6KHz
a–g	0°	0.1522	0.3408	0.7501	0.0755	0.1687	0.3742	0.0168	0.0401	0.0948
	90°	0.1303	0.3374	0.7450	0.0657	0.1671	0.3725	0.0162	0.0429	0.1071
b–c	0°	0.2952	0.4295	0.2062	0.1730	0.2289	0.0938	0.0801	0.0668	0.0061
	90°	0.3067	0.2362	0.0559	0.1844	0.1021	0.0090	0.9171	0.0004	0.0584
b–c–g	0°	0.2870	0.2544	0.0925	0.1590	0.1208	0.0385	0.0627	0.0190	0.0038
	90°	0.2537	0.2880	0.1832	0.1417	0.1375	0.0844	0.0574	0.0239	0.0093
a–b–c–g	0°	0.1719	0.2196	0.1614	0.1510	0.1155	0.0741	0.0602	0.0214	0.0064
	90°	0.2719	0.2441	0.1615	0.1510	0.1286	0.0740	0.0602	0.0176	0.0064

$24kHz$). The samples of voltages and currents considered are from a two cycles long window of data, starting from the fault inception. Different values of the simulation parameters are shown in Table III. Also, various sampling frequencies for obtaining data were used: 24 kHz, 12 kHz, 6 kHz.

The fault location was tested for the case of time variable fault resistance R_F, also. The waveform of R_F is given in Fig. 7. This is an extremely difficult fault condition to analyze and there is no technique proposed to consider it, so far. Tests performed with variable R_F had other simulation parameters given in Table III.

The fault location, given by equation (16), was derived without any constraints regarding the fault resistance. Tests have confirmed that the accuracy of the fault location technique is not affected by the fault resistance. Thus, results obtained for $R_F = 50\Omega$ are given in Tables VI. It was observed that for a given type of fault, the incidence angle does not much influence the error of fault location. The variation of the error due to

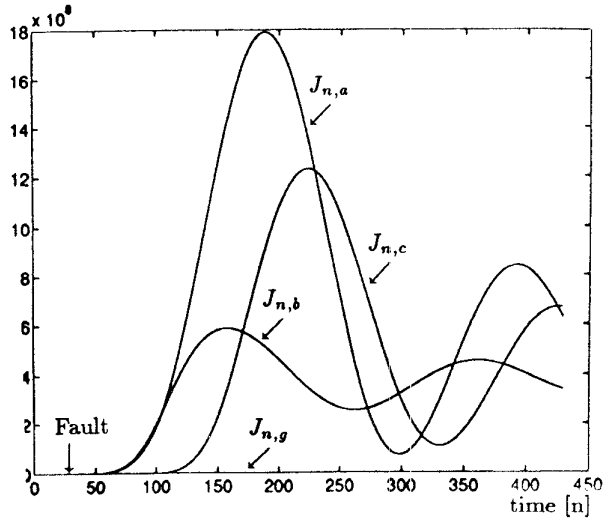

Fig. 5. Classification Indicators for a–b–c–g Fault

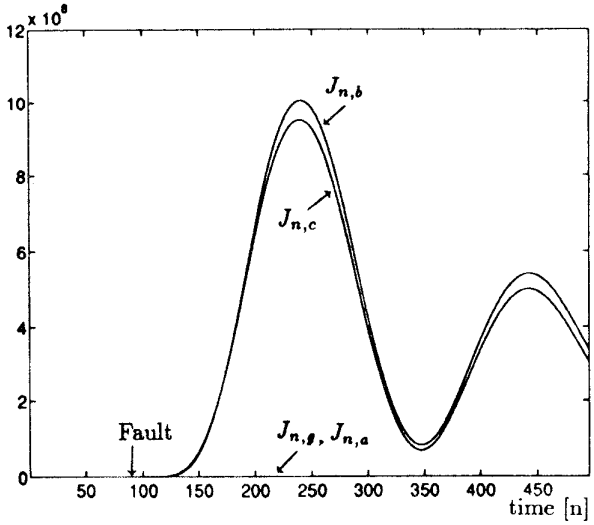

Fig. 6. Classification Indicators for b–c–g Fault

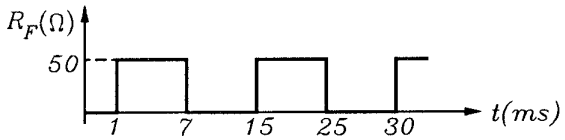

Fig. 7. Variable Resistance R_F

the change in incidence angle increases with a decrease in sampling frequency. Nevertheless, this variation is at most 0.15%. For a particular sampling frequency, the error of the fault location may vary from one fault type to another. Vice versa, for one type of the fault, the error differs with sampling frequency.

Knowing that the approximation of the derivative is a source of error and that it is directly related to the sampling frequency, it was expected that the error would increase as the f_s decreases. Still, such a trend was not observed for cases with constant R_F. It may be concluded that for sampling frequencies used and a constant R_F the approximation of the derivative is good enough. However, for cases with variable R_F, the error increases as sampling frequency decreases. This is due

Table VII. Error (%) for Location 10%, Time Variable Resistance R_F

Type of the Fault	Frequency (kHz)		
	24	12	6
a–g	0.1330	0.6969	2.2398
b–c	0.2736	0.4380	1.5619
b–c–g	0.2537	0.2880	0.1832
a–b–c–g	0.2719	0.2441	0.1615

to the presence of high frequencies in signals at both line ends. These high frequencies are introduced by the abrupt change in R_F. This suggests that the error of the fault location corresponds mainly to the error of the line model. The error obtained with the proposed method for a constant R_F is less than 0.5% in all cases; it is of the same order (sometimes smaller) than in the cited references.

The results for a variable R_F are given in Table VII. The error obtained for $f_s = 6kHz$ is too large. However, the error for $f_s = 12kHz, 24kHz$ can be compared with one for constant R_F. Due to demonstrated robustness regarding various transmission line operating conditions and fault characteristics, it is likely that this method will give better results for the field data tests than the existing ones.

CONCLUSIONS

The results presented in this paper lead to the following conclusions:

- The technique proposed in this paper is based on an off–the–shelf recording instrument incorporating GPS receiver providing synchronized sampling at two ends of a transmission line, which significantly improves quality of data.
- Due to availability of synchronously sampled data, a unique time domain approach for fault analysis was proposed.
- The new fault analysis approach is extremely fast, selective and accurate providing, at the same time, low sensitivity to sources of errors coming from a variety of power system conditions.
- Automated fault analysis using synchronized sampling offers improved performance over known techniques published so far.

ACKNOWLEDGEMENTS

The authors wish to acknowledge financial support for Dr. Peruničić that came from the NASA grant administered by the Center for Space Power at Texas A&M University. Also, the same support was provided to Ms. J. Mrkić who has performed all the programming and testing related to the implementations and simulations presented. Thanks are also due to Dr. A. D. Patton and Dr. F. E. Little from the Center for Space Power for their interest in, and support of, this project.

REFERENCES

[1] T. E. DyLiacco, T. J. Kraynak, Processing by Logic Programming of Circuit Breaker and Protective Relaying Information," *IEEE Trans. on Power Apparatus and Systems*, Vol. PAS–88, No. 2, February 1969.

[2] M. Kezunović, P. Spasojević, C. W. Fromen, D. R. Sevcik, "An Expert System for Substation Event Analysis," *IEEE Transactions on Power Delivery*, Vol. 8, No. 4, October 1993.

[3] M. Kezunović, I. Rikalo, C. W. Fromen, D. R. Sevcik, "Expert System Reasoning Streamlines Disturbance Analysis," *IEEE Computer Applications in Power*, Vol. 7, No. 2, pp. 15–19, April 1994.

[4] M. Kezunović, I. Rikalo, D. J. Sobajic, "Neural Network Applications to Real–Time and Off–Line Fault Analysis," *Intl. Conf. on Intelligent System Applications to Power Systems*, Montpellier, France, September 1994.

[5] M. Kezunović, J. Mrkic, B. Peruničić,"An Accurate Fault Location Algorithm Using Synchronized Sampling," *Electric Power Systems Research Journal*, Vol. 29, No. 3, May 1994.

[6] M. S. Sachdev and R. Agarwal, "A Technique for Estimating Transmission Line Fault Locations from Digital Impedance Relay Measurements," *IEEE Transactions on Power Delivery*, Vol. 3, No. 1, January 1988.

[7] A. T. Johns and S. Jamali, "Accurate Fault Location Technique for Power Transmission Lines," *IEE Proceedings*, Vol. 137, Pt. C, No. 6, November 1990.

[8] A. A. Girgis, et.al., "A New Fault Location Technique for Two– and Three–Terminal Lines," *IEEE Transactions on Power Delivery*, Vol. 7, No. 1, January 1992.

[9] Macrodyne, Inc., "Phasor Measurement Unit– Model 1690," *Application/Performance Data Sheet*, 1993.

[10] T. Takagi, J.–I. Baba, K. Uemura, T. Sakaguchi, "Fault Protection Based on Traveling Wave Theory: Part I – Theory," *IEEE PES Summer Power Meeting*, Paper No. A77 750–3, 1977.

[11] F. Aoki, Y. Akimoto, K. Uemura, T. Sakaguchi, "Totally Digitalized Control System with Simultaneous Data Sampling and Fault Protection Principle Applied to the System," 6^{th} *PSCC*, Darmstadt, 1979.

[12] EPRI, "Electromagnetic Transients Program (EMTP)," *Version 2, Revised Rule Book*, Vol. 1: Main Program, EPRI EL–4541–CCMP, Palo Alto, California, March 1989.

Mladen Kezunović (S'77, M'80, SM'85) received his Dipl. Ing. Degree from the University of Sarajevo, the M.Sc. and Ph.D. degrees from the University of Kansas, all in electrical engineering in 1974, 1977, and 1980, respectively.

Dr. Kezunović's industrial experience is with Westinghouse Electric Corporation in the U.S.A., and the Energoinvest Company in Sarajevo. He also worked at the University of Sarajevo. He was a Visiting Associate Professor at Washington State University during 1986–

has been an Associate Professor at Texas A&M University since 1991. He is a Registered Professional Engineer in the State of Texas.

Branislava Peruničić received her Dipl. Ing. degree in Electrical Engineering from the University of Belgrade, Yugoslavia and Candidate of Sciences Degree in automatic control from the Institute for Automatics and Telemechanics of USSR Academy of Sciences, Moscow in 1960 and 1969, respectively.

Dr. Peruničić was with Energoinvest Company, Sarajevo since 1960. She joined the faculty of the University of Sarajevo in 1964, where she is a Professor of Electrical Engineering. She was a Visiting Research Scholar at the University of Illinois and Texas A&M University in Summer 1993 and Fall 1992/Spring 1993, respectively. She is a member of the Bosnia–Herzegovina Academy of Sciences. Since Fall 1993, she has held a position of Professor at Lamar University.

APPENDIX I

The L_2 norm of a vector is a sum of its squared components. For the case of ΔI_n, the norm is equal to:

$$L_2\{\Delta I_n\} = \sum_m \Delta I_{n,m}^2 \qquad (AI-1)$$

where $\Delta I_{n,m}$ are components of the vector ΔI_n. The average of the norm over last N samples, denoted T_n is equal to:

$$T_n = \frac{1}{N} \sum_{k=n-N+1}^{n} \sum_{m=a,b,c} \Delta I_{k,m}^2 \qquad (AI-2)$$

If the order of the summation is changed, the following expression follows:

$$T_n = \sum_{m=a,b,c} J_{n,m} \qquad (AI-3)$$

where $J_{n,m}$ are averages of squares of fault phase currents:

$$J_{n,m} = \frac{1}{N} \sum_{k=n-N+1}^{n} \Delta I_{k,m}^2 \quad , \quad m = a,b,c \quad (AI-4)$$

These averages are calculated using recursive formulas (12). They have a multiple use: for the fault detection and for the fault classification. This is the reason that $J_{n,m}$ are calculated first, and later summed up to obtain fault detection indicator T_n.

APPENDIX II

Table AII–I. Source Impedances

Bus Name	Per–Unit Value (Ω)		Real Value (Ω)
1	Z_0	0.58+ j 6.32	1.503+j 16.382
	Z_1	0.58+ j 11.41	1.503+j 29.576
2	Z_0	0.07+ j 1.07	0.181+ j 2.774
	Z_1	0.04+ j 0.73	0.104+ j 1.892
3	Z_0	0.75+ j 4.07	1.944+j 10.550
	Z_1	0.31+ j 3.04	0.804+ j 7.880

Table AII–II. System Equivalents

Bus Name	Per–Unit Value (Ω)		Real Value (Ω)
1–3	Z_o	119.69+j 188.93	310.248+j 489.725
	Z_1	1.80+ j 11.44	4.666+ j 29.654
1–2	Z_0	∞	∞
	Z_1	12.58+ j 74.00	32.609+j 191.815
2–3	Z_0	39.79+j 100.63	103.140+j 260.843
	Z_1	2.75+ j 18.32	7.128+ j 47.487

Table AII–III. Self Impedances of Transmission Lines

Bus Name	Per–Unit Value (Ω)		Real Value (Ω)
1–3 (#1)	Z_0	8.94+ j 28.34	23.1734+j 73.4601
	Z_1	1.52+ j 9.06	3.9400+j 23.4844
1–3 (#2)	Z_0	8.52+ j 29.23	22.0847+j 75.7671
	Z_1	1.38+ j 8.80	3.5771+j 76.1300
1–3 (#3)	Z_0	8.40+ j 29.37	21.7736+j 76.1300
	Z_1	1.34+ j 8.73	3.47334+j 22.6290
1–2	Z_0	8.42+ j 26.74	21.8255+j 69.3128
	Z_1	1.50+ j 8.47	3.8882+j 21.9551
2–3	Z_0	3.67+ j 12.38	9.5130+j 32.0902
	Z_1	0.67+ j 3.92	1.7367+j 10.1610